NUMERICAL STUDY OF AIR CONDITION SYSTEM USING SOLAR PARABOLIC COLLECTOR

AHMED R. HASAN[a] **KARIM K . EGAB**[b]

[a] **Assist Lecturer , Foundation of Technical Education , Technical institute of AL SAMAWA-**

Department of Mechanical Engineering , mr.ahmedrazaq@yahoo.com

[b] **PhD student in Mechanical engineering , South Carolina university , Columbia – USA , _iraq2000@yahoo.com**

Abstract

This paper present theoretical analysis for a solar refrigeration process to generate cold air for air conditioning by parabolic collector in AL-Samawa city conditions . The working fluid in the cooling cycle is water only, which is used as refrigerant fluid. The mathematical description based on the conservation equations of mass, energy, momentum, some gas dynamic equations, and state equations, is made to understand the flow inside the ejector. Engineering equation solver (EES) software is used to solve the nonlinear partial differential equations. The objective of work is to study the performance of solar-ejector conditioning system, on 21st day of July and December months in 2011 according to Al- Samawa climates condition the different from other city is by received solar intensity and the position of the city in longitude and latitude lines . The results of performance of the system show that the coefficient of performance between (0.05-0.33) with cooling capacity between (0.1-0.56)KW during the day for a collector of 10.5 m^2 area.

دراسة عددية لنظام تبريد الهواء باستخدام مجمع الطاقة ذو شكل قطع مكافئ

احمد رزاق حسن **كريم خزعل عكاب**

المعهد التقني / السماوة **جامعة ساوث كارولاينا/ الولايات المتحدة**

الخلاصة

تم في هذا العمل دراسة نظرية لمنظومة تبريد تعمل بالطاقة الشمسية باستخدام مجمع شمسي ذي القطع المكافئ الوعائي في مدينة السماوة. تم استخدام الماء كمائع مستخدم في دورة التبريد في المنظومة. اعتمد النموذج الرياضي للمنظومة على معادلات الزخم والكتلة والطاقة ومعادلات الغاز الحركية ومعادلة الحالة لفهم وتفسير جريان المائع داخل القاذف الذي يمثل قلب دورة التبريد.استعملت برمجيات (EES) لحل المعادلات التفاضلية الجزئية اللاخطية. ان الغرض من هذه الدراسة هو تقييم اداء المنظومة خلال يوم 21 من شهر تموز وكانون الاول لعام 2011 حيث تم تصميم وتحليل هذه المنظومة وفقا لظروف مناخ مدينة السماوة حيث يختلف المناخ من مدينة الى اخرى بكمية الاشعاع الشمسي المستلم

Received at28/10/2012** ** Accepted at 29/9/2013**

وموقعها بالنسبة لخطوط الطول والعرض . أوضحت النتائج التي تم الحصول عليها ان معامل اداء المنظومة يتراوح بين (0.33-0.05) ومع حاصل تبريد بين (0.1-0.65) كيلواط بالنسبة لمنظومة تعمل بمجمع شمسي واحد وبمساحة 10.5 م^2

Nomenclature

$A_{s,1}$: cross-section area inside the tube (m^2)

A_s : cross-section area of the absorber (m^2)

A_{env} : cross-section area of the glass envelope (m^2)

C_p : specific heat at constant pressure (J/Kg K)

COP : coefficient of performance

D : The sun's declination angle (Deg)

h : Specific enthalpy (J/kg)

I : solar radiation (W/m^2)

m : mass flow rate (kg/)

M : Mach number

P : pressure (N/m2)

$Q_{in.}$:The total heat transfer between the absorber and the glass envelope (W/m)

$Q_{ex.}$: The total heat transfer between the glass envelope and the environment (W/m)

Q_{gained} : The heat transmitted between the absorber and the heat transfer fluid (W/m)

$Q_{env,abs.}$: The absorbed solar energy by glass envelope (W/m)

$Q_{s,abs.}$: The absorbed solar energy by absorber tube W/m

R : universal gas constant (kJ/kg K)

T : Temperature K

U : velocity m/s

$\dot{V}_f$: Volumetric flow rate of the heat transfer fluid (m^3/s)

v_{wind} : Wind speed (m/s)

n : The day number of the year

W : pump work

W : Aperture width of collector

Greek-Symbols

η Efficiency

θ : Angle of incidence Degree

θ_z : Zenith angle Degree

θ_z : Zenith angle Degree

ε : Effectiveness

ξ : Transitivity of the glass tube

ρ : The density kg/m^3

τ : The solar time or ratio (T_e/T_g) hr

φ : The hour angle degree

ω :M ass ratio , entrainment ratio

α : Absorptivity

γ : Reflectivity of the reflecting surface

δ : Collector optical factor

Subscript

Abs : Absorbed solar energy

c : Cold fluid side

col : Collector

d : Diffuser

e : Evaporator

f :The heat transfer fluid

env : The glass envelope

s :The absorber tube

t : throttle

g : Steam generator

I :inlet

L: Load ,hot fluid side

m : Mixture

no: Nozzle

o : Outlet

st : Storage tank

y : at Section y-y

1. Introduction

The solar-driven ejector refrigeration system appear as an attractive alternative for refrigeration technologies due to its capacity to use low temperature heat supply. It major component include solar collectors, a hot oil storage tank, an ejector cycle as shown in Fig.(1)

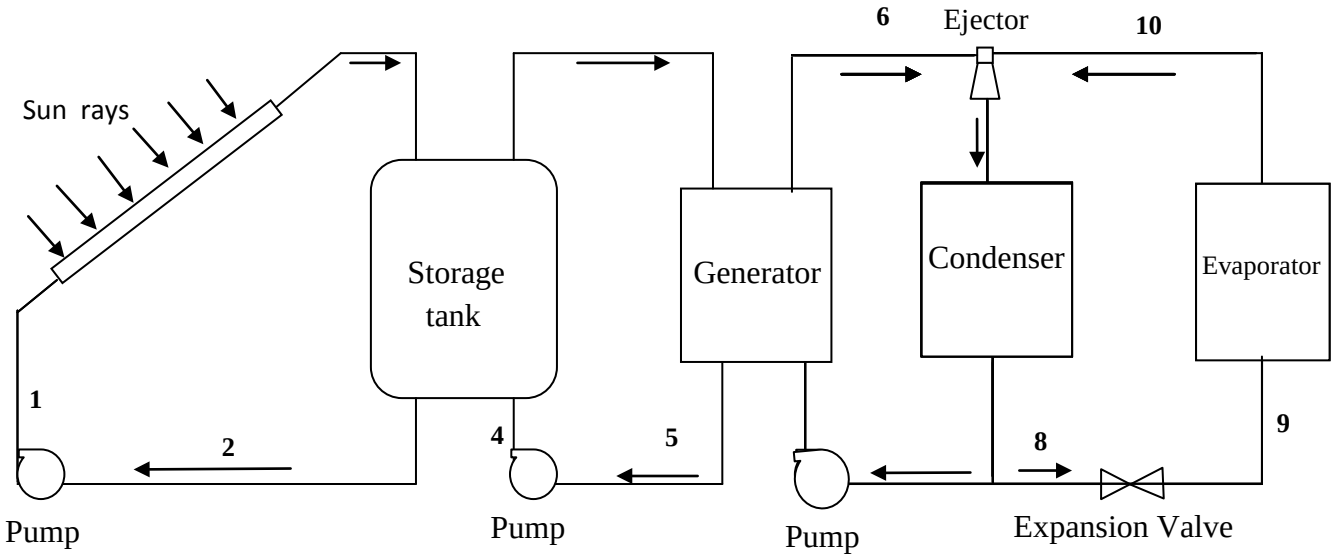

Fig.(1) : Solar – air conditioning system diagram

The collector pump circulates oil between the collector and the storage tank. The oil conveys heat from the collector to the storage tank. Then, hot oil from the storage tank is carried to the generator where the refrigerant vaporizes. When the heat provided by the storage tank is not sufficient, may the auxiliary pre-heater acts as an additional source of energy to ensure that pressure and temperature conditions required by the ejector are achieved. The high pressure primary vapor flow is generated and the low pressure vapor flow of the refrigerant coming from the evaporator is induced to the ejector. The primary and the secondary vapor stream are mixed at the mixing section where an aerodynamic shock is included to create a compression effect. The mixed stream is then discharged, via a diffuser, to a condenser rejecting heat at ambient temperature to the cooling water system. Then, the refrigerant flows through an expansion valve to the evaporator, where it absorbs heat at low temperature from chilling water. The remaining liquid refrigerant is pressurized by refrigerant pump and vaporized in the generator using heat from the solar collector system, thus completing the cycle as shown in Fig.(1) This work gives particular attention to the use of an ejector in the cooling cycle, due to it is construction simplicity, absence of moving parts, operation at low temperature and a

low operational cost, being attractive for refrigeration and air conditioning applications. It has been shown that the cooling cycle performance.

2. Literature review

A number of studies can be found in the literature concerning solar ejector cooling system . A theoretical work on solar air conditioning system can be found in ***Hung et al. 1985 [1]***, developed a high –performance solar ejector refrigeration system using R141b as the working fluid. They obtained a coefficient of performance of a single- stage ejector cooling system around 0.22 at a generating temperature of 95C^o, condensing temperature of 32 C^o and evaporating temperature of 8C^o, and solar radiation of 700 W/m^2. Water was used as the refrigerant in the modeling study presented by ***Khattab and Barakat in2002 [2].*** Very low generator temperature (50 C^o) and cooling load (0.4 kw) were considered. ***In 2006, Vidal et al. [3]***, analyzed the solar ejector cycle using R-141b as its working fluid by using the TRNSYS and engineering equations solver (EES) simulation tools. The system was designed to deliver 10.5 kw of cooling with 80 m^2 of flat-plate collector, and 4 m^3 of hot-water storage tank. They reported the maximum COP of 0.22 at a generating temperature of 80 C^o, an evaporating temperature of 8C^o , and condensing temperature of 32C^o. ***in 2009, Clemens Pollerberg et al. [4]***, present experimental work by design a system of a solar driven air conditioning system, with water as working fluid in the system, a designed cold capacity was 1 kw, the investigation shows that the cooling water temperature as well as the cold water temperature has strong influence on the coefficient of performance of a steam jet ejector.

3. Theoretical analysis

Detailed information about solar radiation availability at any location is essential for the design and economic evaluation of a solar energy system . its known as direct solar radiation on a surface depends on the sun's position in the sky . the sun's position is a function of the latitude (l) , the solar declination (d) , and the hour angle (φ) .from the fundamentals of solar geometry , these parameters are given by [6];

$$d = 23.5\sin\left(\frac{360}{365}(284+n)\right) \text{ [Degrees]} \qquad (1)$$

Where (n) is the day of the year.

$$\varphi = 15\ (\tau - 12) \tag{2}$$

$$\cos(\theta_z) = \cos(l)\cos(d)\cos(\varphi) + \sin(l)\sin(d) \tag{3}$$

The incident angle θ of solar beams on a surface is given by :

$$\cos(\theta) = \left[\cos^2(\theta_z) + \cos^2(d)\sin^2(\varphi)\right]^{1/2} \tag{4}$$

The solar intensity on a surface is given by [7] ;

$$solar\ \ beam\ \ radiation\ \ component\ = I_{DN}.\cos(\theta) \tag{5}$$

A and **B** are monthly dependent parameters tabulated [7] .

3.1 Solar intensity in AL SAMAWA City

As mentioned previously , the solar intensity can be calculated using equations 1 to 4 . its noted that the solar incidence on a surface depends on three important variables : the solar declination (d) , the latitude (l) and the time (τ) . equation (5) represents the final equation where the solar incidence radiation for any location can be calculated .

3.2 Collector model

The sun's energy, reflected by the mirror, fall on the absorber after passing through the glass envelope . the differential equations for the temperatures of the HTF, the absorber and the glass envelope are established. The differential equations are coupled through relations for the heat transfer between the different parts of the heat collection element. To derive the appropriate differential equations. The heat collection element consists of the absorber pipe in which the HTF flows. A glass envelope covers the absorber pipe.

A Transient energy balance for the HTF leads to the following partial differential equation for the HTF temperature [8]:

$$\rho_f\ c_{P,f}\ A_{s,1}\ \frac{\partial T_f}{\partial\ t} = -\rho_f\ c_{P,f}\ \dot{V}_f(t)\ \frac{\partial T_f}{\partial z} + Q_{gained} \tag{6}$$

The distance along the collector is *z*, and *t* is the time. The boundary condition for equation (6) is:

$$T_f(0,t) = T_{f,i}(t) \tag{6 a}$$

with $T_{f,i}$ as the HTF collector inlet temperature. The initial condition for equation (6) is:

$$T_f(z,0) = T_{f,0} \qquad (6\ b)$$

The differential equation for the absorber temperature is given through [8]:

$$\rho_s\ c_{P,s}\ A_s \frac{\partial T_s}{\partial t} = Q_{s,abs.} - Q_{in.} - Q_{gained} \qquad (7)$$

The initial condition for equation (3.11) is:

$$T_s\ (z,0) = T_{s,0} \qquad (7\ a)$$

The differential equation for the envelope temperature is given through [8]:

$$\rho_{env}\ c_{P,env}\ A_{env}\ \frac{\partial T_{env}}{\partial t} = Q_{env,abs.} + Q_{in.} - Q_{ex.} \qquad (8)$$

The initial condition for equation (8) is:

$$T_{env}(z,0) = T_{env,0} \qquad (8\ a)$$

The interacting dynamic of the temperatures given through the differential equations (6), (7) and (8) is determined by the heat transfer between the HTF, the absorber, and the envelope.

the solar absorption in the glass envelope becomes [7]:

$$Q_{env,abs.} = \gamma \alpha_{env} \delta w I_{DN} \cos(\theta) \qquad (9)$$

While , the equation for the solar absorption in the absorber becomes [7]:

$$Q_{s,abs} = \gamma \xi \alpha_s \delta w I_{DN} \cos(\theta) \qquad (10)$$

(Q_{gained}), ($Q_{in.}$) and ($Q_{ex.}$) values can determined from heat balance for the element of collector pipe . finally, the collector outlet temperature ($T_{f,o}$) is calculated by solving the nonlinear differential equations ODE (6) ,(7) and (8) using numerical solution (finite difference method) .

3.3 Storage Tank Model

The hot oil outlet from solar collector provide heat to a thermal storage system. The advantage of having a thermal storage system is that it can store the thermal energy generated

during the peak radiation hours for later use when solar radiation is unavailable. A full mixing model is assumed in order to simplify the energy balance of the system all the fluid inside the storage tank is considered to be at the same temperature, the storage tank diagram as shown in Fig.(2) , and the system pipes are ideal, without friction and storage tank is also insulated.

For insulated storage Tank the equation above becomes :

$$\left(\dot{m}\ c_P\right)_{st}.\frac{dT_{st}}{dt} = \dot{m}_f\ c_{P,f}\left(T_{f,o} - T_{st}\right) - \dot{m}_L\ c_{P,f}\left(T_{L,i} - T_{L,o}\right) \qquad (11)$$

With initial condition ,

at t=0 $\qquad T_{st} = T_a$ (11 a)

In order to find T_{st} ,Eq.(11) solved numerically for each time step (Δt) .

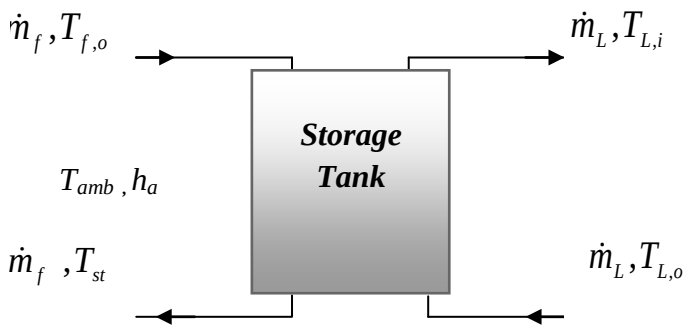

Fig. (2) : Storage Tank diagram

3.4 Steam generator Model

Generator vapour is a heat exchanger connected between solar heat system and ejector cooling system as shown in Fig.(3), and operate as a heat source to the ejector cooling cycle .The model of generator is based on effectiveness-NTU method [9].

By considering overall energy balances for the hot and cold fluids, the total heat transfer rate is obtained as,

$$q = \varepsilon C_{\min}\left(T_{L,i} - T_{c,i}\right) \qquad (12)$$

For any heat exchanger, ε is a function of two parameters, which are NTU and C_r :

$$\varepsilon = f(\text{NTU}, C_r) \qquad (12\ a)$$

The effectiveness ε is given as [41]:

$$\varepsilon = \frac{1 - \exp\left[-NTU\left(1 - C_r\right)\right]}{1 - C_r\ \exp\left[-NTU\left(1 - C_r\right)\right]} \qquad (12\ b)$$

Where, NTU is the number of transfer units, defined as ,

$$NTU = \frac{U A}{C_{\min}} \qquad (12\ c)$$

C_r is the heat capacity ratio, defined as ,

$$C_r = \frac{C_{\min}}{C_{\max}} \qquad (12\ d)$$

Where , $C_{max} = Cc$ or C_L, whichever is larger . (12 e)

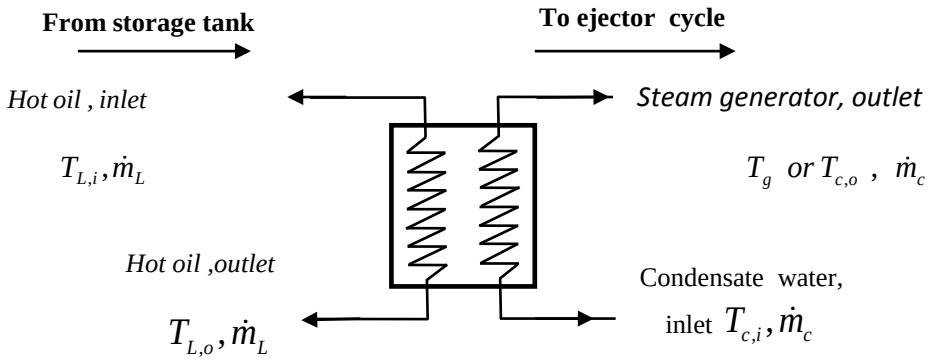

Fig.(3) : Flow diagram of steam generator

3.5 Ejector Model

An ejector is a device in which a higher pressure fluid (also called primary fluid) is used to induce a lower pressure fluid (called secondary fluid) into the ejector . As shown in Fig .(4) ,The high pressure primary steam starts to accelerate as it enters a convergent section of the nozzle and reaches the sonic level at the nozzle throat section (1-1). The speed of primary flow is further increased while expanding through a divergent section of the nozzle. At the exit plane section (2-2), the primary fluid expands out with supersonic speed and results the low pressure region section (2-2). This pressure is lower than the pressure in the evaporator and allows a liquid refrigerant in the evaporator to vaporize at low temperature to create the refrigeration effect (Heat used to vaporize this refrigerant is the cooling load of the system) .

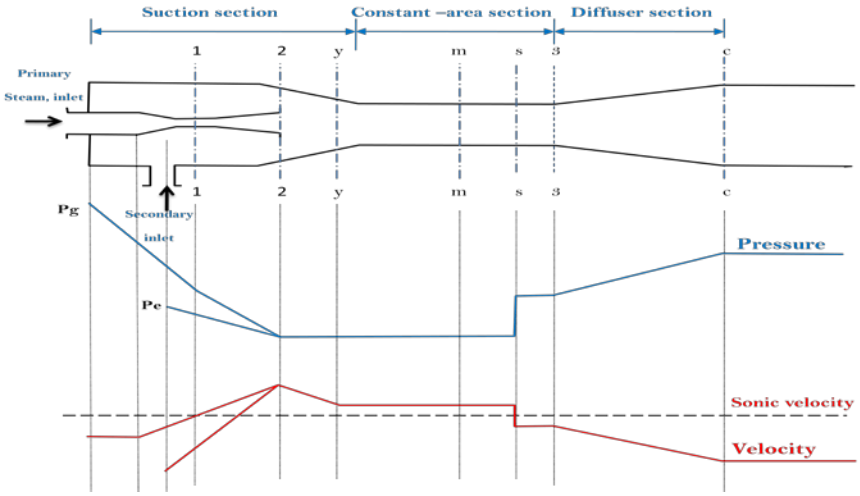

Fig .(4) Variation in steam pressure and velocity along the ejector [10]

The evaporated ‘‘secondary fluid’’ will be entrained from the evaporator and flow out without mixing with primary fluid immediately . Both fluids assumed that to be start mixing somewhere at the downstream of the nozzle exit section (y-y) in the suction chamber ,then the mixing stream enter the constant area at section (m-m). A normal shock wave is then induced in the ejector throat section (s-s), creating a compression effect, and the flow speed suddenly drops to subsonic value. Further compression is achieved when the mixed stream passes through the subsonic diffuser (d) [11].

The following assumptions are made for the analysis :

1-The process in the ejector to be adiabatic and the flow inside the ejector is assumed to be steady and one dimension..

2- Kinetic energy of the inlet and outlet flows is neglected .

3- Friction and mixing loss is accounted in the form of isentropic efficiency.

5- The working fluid is an ideal gas with constant properties c_p and γ .

6-The two streams starts to mix at the cross section y–y with a uniform pressure, at suction chamber before the shock which is at the cross section s–s .

7 - The constant-pressure mixing occurred at the inlet of the constant area section .

3.5.1 Governing equations

Under ideal condition ,the general governing equations for the suction ,constant area and diffuser are as the follow [10] :

Conservation of momentum $$P_i A_i + \sum m_i u_i = P_o A_o + \sum m_o u_o \quad (13)$$

Conservation of energy $$\sum m_i \left(h_i + u_i^2 / 2\right) = \sum m_o \left(h_o + u_o^2 / 2\right) \quad (14)$$

Conservation of mass $$\sum \rho_i u_i A_i = \sum \rho_o u_o A_o \quad (15)$$

Definition of Mach number $$M = \frac{u}{c} \quad ; \quad c = \sqrt{\gamma R T} \quad (16)$$

A- Primary flow through nozzle (section 1-1)

For a given inlet stagnant pressure P_g and temperature T_g , the mass flow through the nozzle at choking condition is given as :

$$\dot{m}_g = \frac{P_g A_1}{\sqrt{T_g}} \sqrt{\frac{\eta_{no}\,\gamma}{R}\left(\frac{2}{\gamma+1}\right)^{(\gamma+1)/(\gamma-1)}} \quad (17)$$

where η_{no} is a coefficient relating to the isentropic efficiency of the compressible flow in the nozzle.

B- Nozzle - Suction chamber (section 2–2)

The gas dynamic relations between the Mach number at the exit of nozzle M_2 and the exit cross section area A_2, using isentropic relations as an [12]:

$$\left(\frac{A_2}{A_1}\right)^2 = \frac{1}{M_{g2}^2}\left[\frac{2}{\gamma+1}\left(1+\frac{(\gamma-1)}{2}M_{g2}^2\right)\right]^{(\gamma+1)/(\gamma-1)} \quad (18)$$

And ,the relation between primary Mach number at exit nozzle and pressure at nozzle exit P_2 is given as :

$$\left(\frac{P_g}{P_2}\right) = \left(1+\frac{(\gamma-1)}{2}M_{g2}^2\right)^{\gamma/(\gamma-1)} \quad (19)$$

While, the relation between secondary Mach number nozzle exit and pressure at nozzle exit P_2 is :

$$M_{e2} = \sqrt{\frac{2}{\gamma - 1}\left[\left(\frac{P_e}{P_2}\right)^{\left(\gamma-1/\gamma\right)} - 1\right]} \tag{20}$$

C- constant area section

The mixing process is modelled by one-dimensional continuity, momentum and energy equations. This section include the following subsections :

1-Mixing section (*m-m*)

These equations are combined to define the critical Mach number of the mixture at point ***m*** in terms of the critical Mach number for the primary and entrained fluids at point 2 , based on assumption 4 and 7, the momentum eq.(14) between section 2-2 and *m-m* can be simplified into [13] :

$$\eta_m\left(\dot{m}_g u_{g2} + \dot{m}_e u_{e2}\right) = \left(\dot{m}_g + \dot{m}_e\right) u_m \tag{21}$$

with η_m as the efficiency for the whole mixing chamber .

by using Eq.(16) and Eq.(21) then the Mach number of two streams at constant pressure is given as [12] :

$$M_m^* = \frac{M_{g_2}^* + \omega\, M_{e_2}^* \sqrt{\tau}}{\sqrt{((1+\omega\tau)(\omega+1))}} \tag{22}$$

The relationship between *M* and M^* at any point in the ejector is given by this equation [13]:

$$M^* = \sqrt{\frac{M^2(\gamma+1)}{M^2(\gamma-1)+2}} \tag{23}$$

Eq.(23) is used to calculate M^*_{e2} , M^*_{g2} ,M_m .

2-Mixed flow across the shock section (*m–m to 3–3*)

A supersonic shock will take place at section *s–s* with a sharp pressure rise. Assuming that the mixed flow after the shock undergoing an isentropic process, the mixed flow between

section *m–m* and section 3–3 inside the constant area section has a uniform pressure P_3.Using normal shock relation , the Mach number of the mixing after the shock wave is :

$$M_3 = \sqrt{\frac{M_m^2 + \left(\frac{2}{\gamma - 1}\right)}{\left(\frac{2\gamma}{\gamma - 1}\right) M_m^2 - 1}} \tag{24}$$

The pressure after the shock wave can be calculate from the following relation :

$$\frac{P_3}{P_m} = \frac{1 + \gamma M_m^2}{1 + \gamma M_3^2} \tag{25}$$

D- Mixed flow through diffuser

After passing through the constant area throat section from section (*m-m*) to section (*3-3*) the flow is expanded through a diffuser with a given isentropic efficiency to the condenser pressure ,The pressure at the exit of the diffuser follows the relation, assuming isentropic process :

$$\frac{P_d}{P_3} = \left(1 + \frac{\eta_d (\gamma - 1)}{2} M_3^2\right)^{\gamma/(\gamma-1)} \tag{26}$$

The area ratio of nozzle throat and diffuser constant area is given as [12]:

$$\frac{A_1}{A_3} = \frac{P_d}{P_g}\left(\frac{1}{(1+\omega)(1+\omega\tau)}\right)^{1/2} \frac{\left(\frac{P_2}{P_{d.}}\right)^{1/\gamma}\left(1 - \left(\frac{P_2}{P_{d.}}\right)^{(\gamma-1)/\gamma}\right)^{1/2}}{\left(\frac{2}{\gamma+1}\right)^{1/(\gamma-1)}\left(1 - \frac{2}{\gamma+1}\right)^{1/2}} \tag{27}$$

3.5.2 Performance of the ejector cycle

The performance of a refrigeration cycle is generally expressed through the coefficient of performance, which is the output cooling power for a unit energy input:

$$COP = \frac{Q_e}{Q_g + W} \tag{28}$$

Also there is another performance element it is the mass flow ratio between the evaporator and generator streams , called the entrainment ratio (ω) :

$$\omega = \frac{\dot{m}_e}{\dot{m}_g} \tag{29}$$

3.6 Condenser

The condenser is an indirect contact heat exchanger in which total heat rejected from the refrigerant fluid is removed by a cooling medium like air.

The energy conservation in the condenser could be calculated as follows:

$$Q_{cond} = \dot{m}_{cond} \, (h_3 - h_4) \tag{30}$$

Where , $\dot{m}_{cond.} = \dot{m}_g + \dot{m}_e$ (30 a)

3.7 Evaporator Model

The evaporator in ejector refrigeration system **ERS** which is a vessel content the water that will evaporate by subjecting liquid water to a pressure below the saturation pressure corresponding to the temperature to which the water will be cooled. Fig.(5) shows schematic of evaporator only a small fraction of the water's mass need be evaporated for an appreciable temperature reduction, due to the high enthalpy of vaporization of water. [**13**].

The cooling capacity in the evaporator is given by :

$$Q_e = \dot{m}_e (h_{10} - h_9) \tag{31}$$

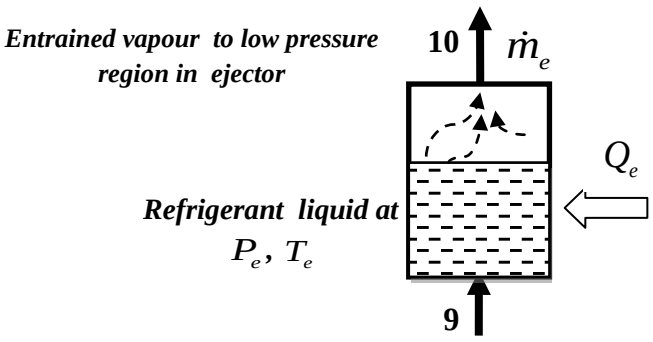

Fig.(5) Schematic representation of evaporator

4. Result and discussion

Figures (6 ,7) shows the direct normal radiation and its component (incidence radiation) for the summer month July and winter month December , with a sine profile behavior, which reach a maximum value in range around (850-900 W/m^2) in mid-day, as demonstrated in its noted that the values of the direct normal radiation and its component are very close to each other in July , because the tilting of incident solar radiations are small in summer seasonal, therefore, the maximum values of their useful solar radiation are about in the range (985-900 W/m^2) in summer months.

Figures (8, 9) shown the solar energy in July and winter month December, increases from zero before sunrise time, and then a best value occurs at (12:00 p.m.) depending on the component of direct normal radiation, after that decreases progressively to zero at sunset. It can be seen from these two figures that the absorbed energy by tube reaches to value above (3000 W/m) I July while it reach to value above (2000 W/m) at period from (9:00 a.m.) to (15:00 p.m.)

Figures (10,11) , represent the collector outlet temperature behavior in July and December the value increase from value equal to ambient temperature at (5:00 a.m.) to reach maximum value about (163 C^o) on July while in December reach to (135 C^o) at (12:00 p.m.) then the collector outlet temperature is about (40 C^o) at (12:00 a.m.) depending on the absorbed solar energy.

Figures (12,13), shown the value of storage tank temperature vs. time for July and December , is reached slightly to a maximum value during period from (13:00 p.m.) to (18:00 p.m.) according to the value of collector outlet temperature, while after sunset it take to decrease in value at mid-night.

Figures (12,13) , also demonstrated the generator outlet temperature in July and December beginning before sunshine with value about (24C^o) closed to ambient temperature, then the temperature of generator was increase step by step with the sunshine due to increase in storage tank temperature to reach maximum value to about (125C^o) in July while in December is about (110 C^o) at (16:00 p.m.), then the temperature was taken in decrease slowly after sunset to reach to its value about (100 C^o) in July at (23:00 p.m.).

Figures (14,15) , shows the entrainment ratio (*w*) and coefficient of performance (COP) vs. time for July and December , as it is clear from figures that the (COP) and (*w*) start with value below (0.05) at (5:00 a.m.) and then when sun rise the values rise to reach maximum values (COP) and (*w*), respectively at period from (12:00 p.m.) to (20:00 p.m.) because of generator pressure and temperature above 1 bar in this period, then decrease slowly after sunset according to gradually decreasing in generator pressure and temperature.

Figures (18,19), demonstrated the cooling capacity of system in July and December , start to increase and has maximum value at (16:00 p.m.), then decrease slowly after sun absent depending on generator pressure and temperature and entrained mass flow rate ($\dot{m}_e$) value according to eq.(29).

Figure (16) , shows the COP vs. condenser temperature, as shown from figure the COP increase if condenser temperature decrease, while the COP is decrease if condenser temperature increase because the effect of the condenser temperature on the back pressure and that leads to effect on secondary mass rate value.

Figure (17), shows the COP vs. generator temperature, as its demonstrated from figure, the COP increase with increase generator temperature and vice versa because the increase in temperature leads to increase in pressure that in necessary to create vacuum and entrained the secondary mass from the evaporator.

5. Conclusions

In this study, theoretical analysis model is made for performance prediction of solar-driven ejector refrigeration system for providing air conditioning was studied. The results of the mathematical simulation have demonstrated that the solar-driven ejector refrigeration system can be designed to meet the cooling requirements of air conditioning for houses in Al SAMAWA
city . The following conclusions were obtained :-

(1) It is concluded from the present study that was performed that solar driven air conditioning has practical and economically because it is used free energy when compared to conventional vapour compression air conditioner .

(2) For the studied case, the condenser temperature influences more on the performance of the SERS than the generator temperature.

(3) From 12:00 p.m. to 17:00 p.m. , on typical clear sky days, the average COP of the system is 0.33 with most of the daytime remaining steady between 0.3–0.33, except at 24:00 a.m. , when it
drops as low as 0.28 .

(4) The coefficient of performance COP and cooling capacity QE difference is more noticeable in the summer months than in the winter .

(5) The modeling results of this study give guidance for the possible use of solar energy to driven conditioning application in al Samawa city.

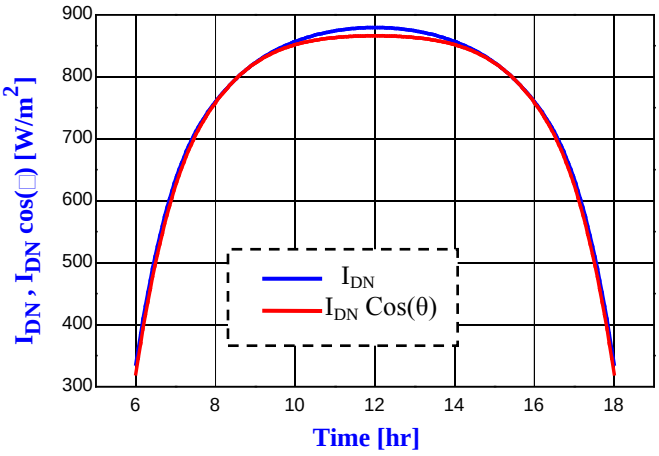

Fig.(6) The Direct Normal Radiation and its component vs. time for samawa city on 21 July 2011

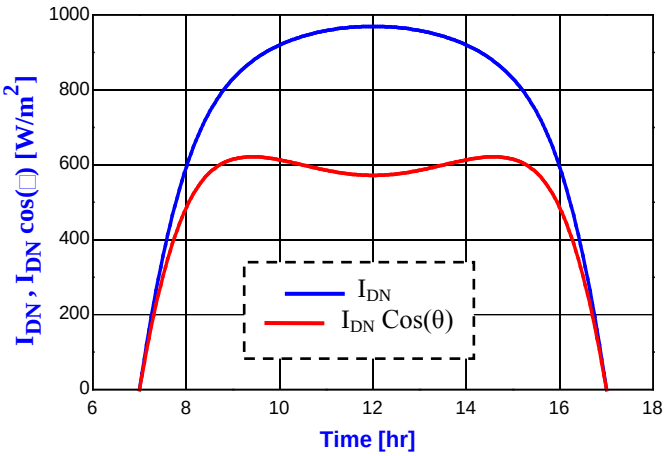

Fig. (7) : The Direct Normal Radiation and its component vs. time for samawa city on 21 December 2011

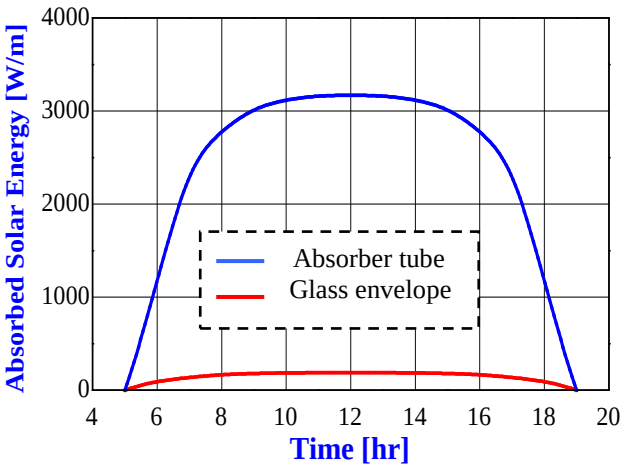

Fig.(8): Absorbed Solar Energy from the solar field for 21 July 2011

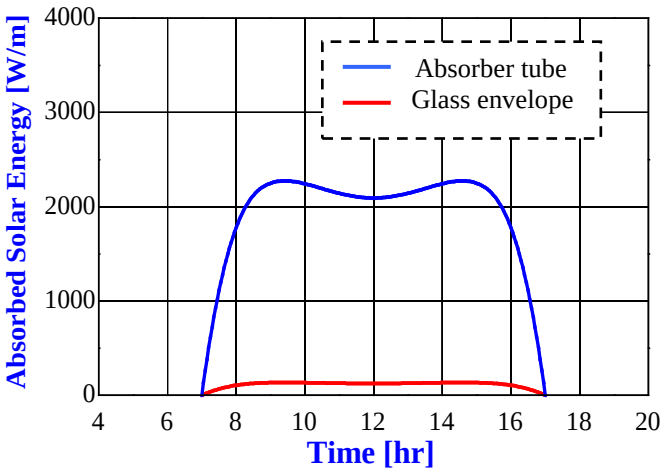

Fig.(9) Absorbed Solar Energy from the solar field for 21 December 2011

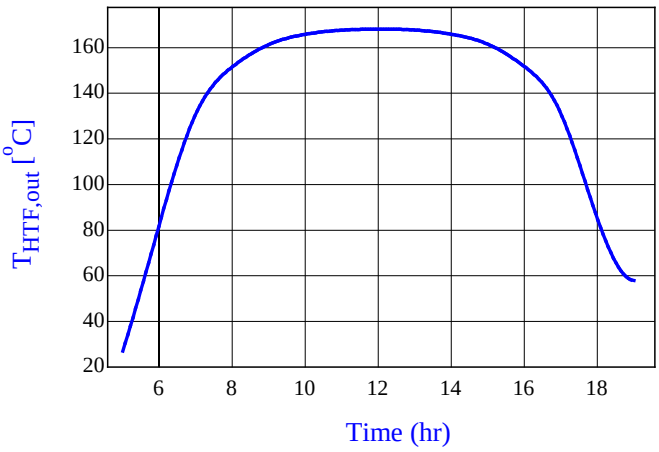

Fig. (10): Collector outlet temperature vs.time for Samawa city on 21 July 2011.

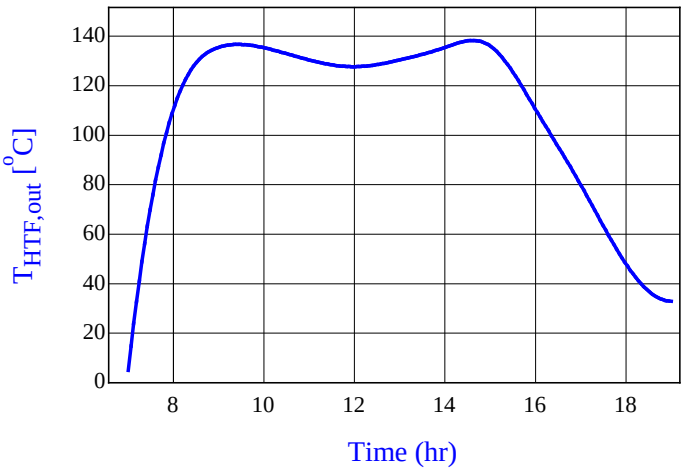

Fig. (11): Collector outlet Temperature vs. time for Samawa city on 21 December 2011

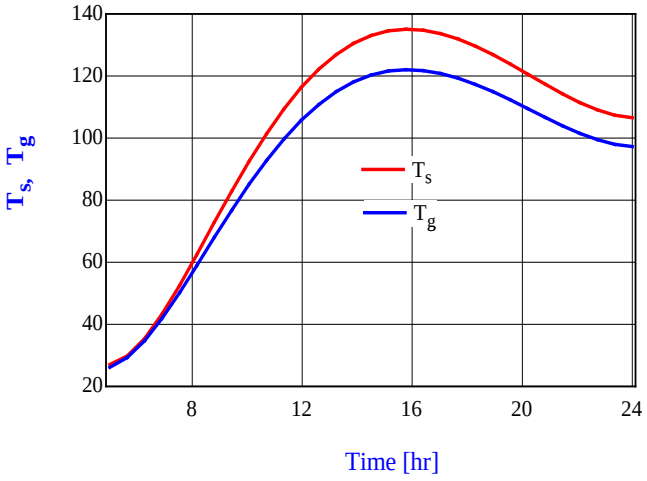

Fig. (12): Storage tank tank and generator Temperatures vs. time on 21 July

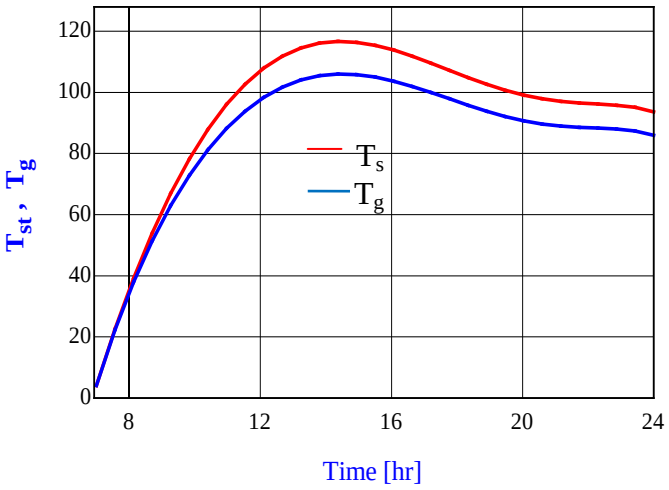

Fig.(13): Storage tank and generator Temperatures vs. time on 21 December

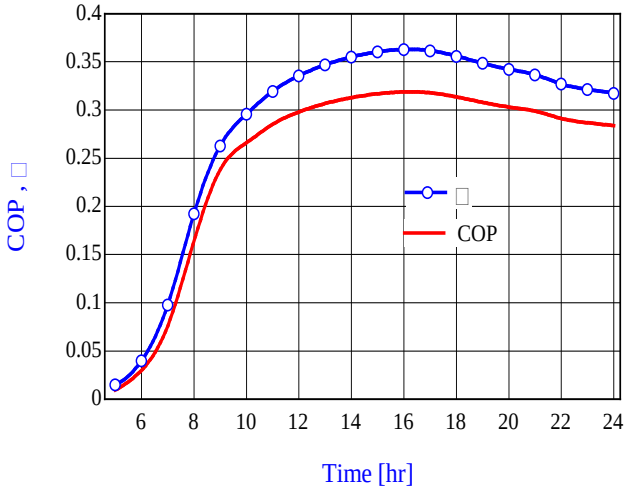

Fig.(14): The Coefficient of Performance and mass ratio vs. time for samawa city on 21 July 2011

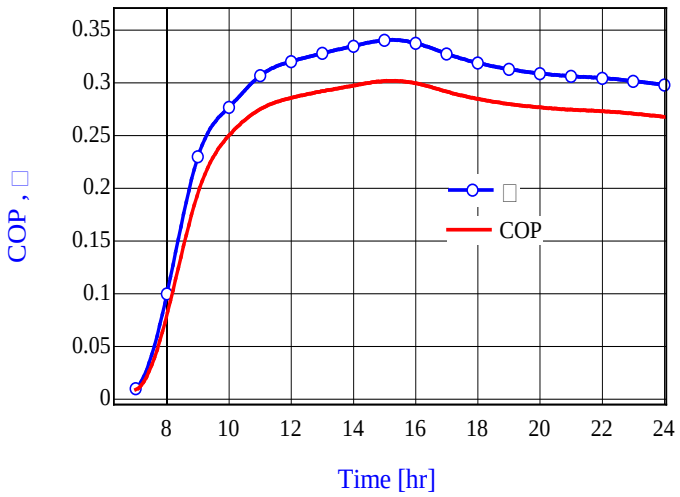

Fig.(15): The Coefficient of Performance and mass ratio vs. time for samawa city on 21 December 2011

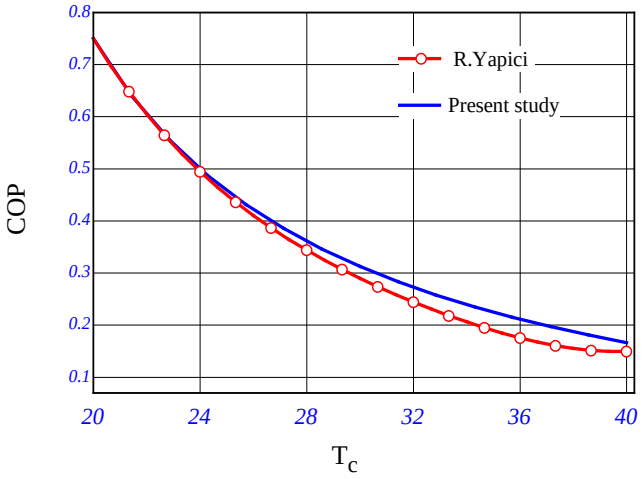

Fig. (16): The effect of the condenser temperature on the optimum COP

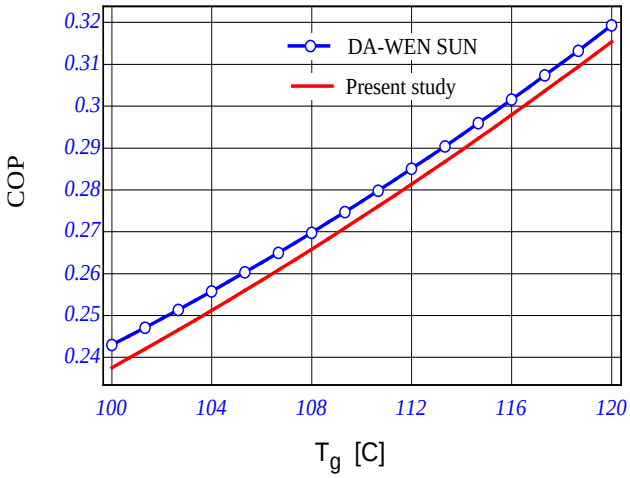

Fig. (17): The effect of the generator temperature on the optimum COP

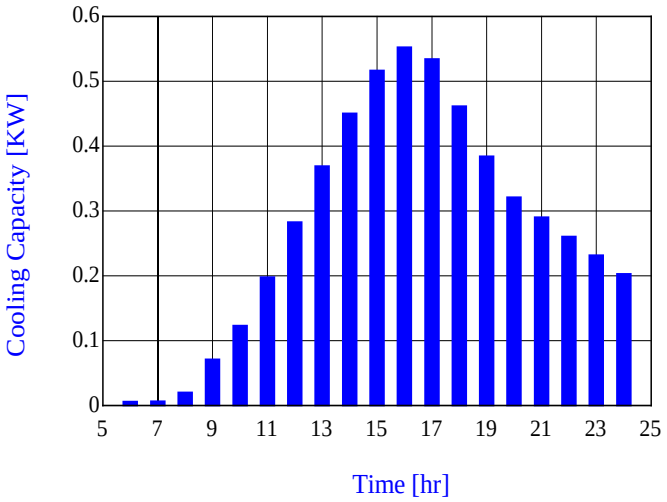

Fig.(18): Cooling Capacity vs. time for Samawa city on 21 July 2011

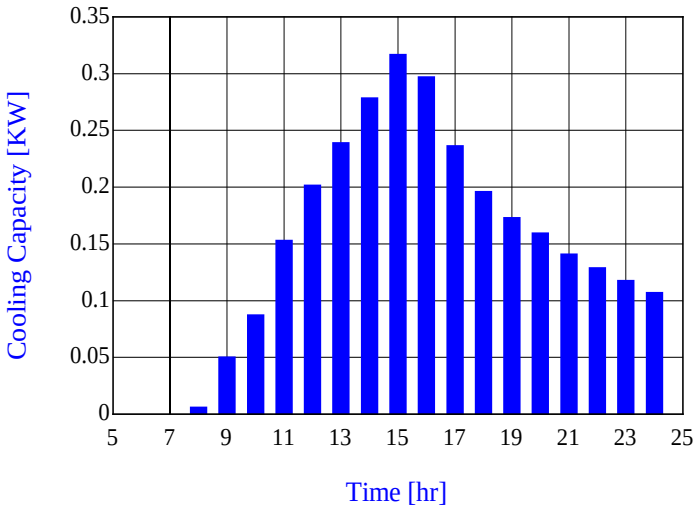

Fig.(19): Cooling Capacity vs. time for Samawa city on 21 December 2011

7. References

[1] Huang B. J., Jiang C. B. and Hu F. L., Ejector performance characteristics and design analysis of jet refrigeration system. ASME J. Eng. Power,107, pp. 792–802 , 1985 .

[2] Khattab N. , Barakat M. , Modelling the design and performance characteristics of solar steam-jet cooling for comfort air conditioner. Solar Energy, pp. 73-257 , 2002 .

[3] Vidal H. , Colleb S. and Pereirab G. 'Modeling and hourly simulation of a solar ejector cooling system' . Applied Thermal Engineering, pp. 26-663, 2006 .

[4] Clemens Pollerberg , Ahmed Hamza H. Ali , Solar driven steam jet ejector chiller , Applied Thermal Engineering , pp.1245–1252, 2009 .

[5] Jiasm .M. Abdulateef, K. Sopian, Mohammd.A. Alghoul , 'Review on solar-driven ejector refrigeration technologies' , Renewable and Sustainable Energy Reviews, No. 13,1338–1349 , 2009.

[6] Salih, M. A., Kaseb, S. and EL-Refaie, M. F., "Glass-azimuth modification to reform direct solar heat gain", J. Building and Environment, vol.39, pp.653-659, 2004 .

[7] ASHRAE handbook of fundamental Atlanta, GA, USA , 1993 .

[8] **Stuetzle, A. , Blair, N., Mitchell, W. J.,** "Automatic Control of a 30 MWe SEGS VI Trough Plant", Solar Energy, Vol. 76, pp. 187-193, 2004.

[9] Navarro H.A. , Cabezas L.C., Effectiveness-NTU Computation With a mathematical Model For Cross-Flow Heat Exchangers , Brazilian Journal of Chemical Engineering ,Vol. 24, No. 04, pp. 509 – 521 , 2007.

[10] Yapıcıa R. , Ersoya H. , Aktoprakoglua A., Experimental determination of the optimum performance of ejector refrigeration system depending on ejector area ratio , international journal of refrigeration , pp. 1183 –1189 , 2008

[11] S. He, Y. Li, R. Z. Wang, Progress of mathematical modeling on ejectors, Renewable and Sustainable Energy Reviewable , pp. 1760-1780 , 2009

[12] Hisham El-Dessouky, Hisham Ettouney, 'Evaluation of steam jet ejectors' , Chemical Engineering and Processing , No. 41 , 551–561, 2002.

[13] M. D. Butterworth, T. J. Sheer, "High pressure water as the driving fluid in an ejector refrigeration system", Applied Thermal Engineering' , No. 27 , 2145-2152 , 2007